

## Measurement of heart rate variability and stress evaluation by using microwave reflectometric vital signal sensing

長江, 大輔  
九州大学産学連携センター

間瀬, 淳  
九州大学産学連携センター

<https://hdl.handle.net/2324/18617>

---

出版情報 : Review of Scientific Instruments. 81 (9), pp.094301-1-094301-10, 2010-09-13.  
American Institute of Physics

バージョン :

権利関係 : © 2010 American Institute of Physics

# Measurement of heart rate variability and stress evaluation by using microwave reflectometric vital signal sensing

Daisuke Nagae and Atsushi Mase

*Art, Science and Technology Center for Cooperative Research, Kyushu University, Kasuga 816-8580, Japan*

(Received 27 April 2010; accepted 19 July 2010; published online 13 September 2010)

In this paper, we present two robust signal processing techniques for stress evaluation using a microwave reflectometric cardiopulmonary sensing instrument. These techniques enable the heart rate variability (HRV) to be recovered from measurements of body-surface dynamic motion, which is subsequently used for the stress evaluation. Specifically, two novel elements are introduced: one is a reconfiguration of the HRV from the cross-correlation function between a measurement signal and a template signal which is constructed by averaging periodic component over a measurement time. The other is a reconstruction of the HRV from the time variation of the heartbeat frequency; this is evaluated by a repetition of the maximum entropy method. These two signal processing techniques accomplish the reconstruction of the HRV, though they are completely different algorithms. For validations of our model, an experimental setup is presented and several sets of experimental data are analyzed using the two proposed signal processing techniques, which are subsequently used for the stress evaluation. The results presented herein are consistent with electrocardiogram data. © 2010 American Institute of Physics. [doi:10.1063/1.3478017]

## I. INTRODUCTION

In recent years, the stress evaluation technique using the heart rate variability (HRV) has been recognized widely as an advanced diagnostic tool to prevent the stress syndrome, for example, sleep sign while driving in a car, etc.<sup>1-3</sup> The HRV is generally obtained from monitoring the peak intervals (R-R intervals) in an electrocardiogram (ECG). However, evaluation of stress by using the ECG is not well suited for long-time monitoring. This is because several electrodes must be attached directly to a human body to acquire the ECG data. In this work, we report new techniques to evaluate the stress using a noncontacting and noninvasive microwave radar reflectometer method.

The measured microwave reflectometer signal consists of the respiration signal, the heartbeat signal, and the random movement of a human body. To extract the heartbeat signal from the measured signal, for example, the respiration signal is removed by a high-pass filter (HPF) with a cutoff frequency of 0.7 Hz, however, the random movement of the human body components, still cannot be removed. The heartbeat signal is very small and has low signal-to-noise (S/N) ratio due to the cardiac movement that appears on the body surface. For these reasons, the peak positions in the heartbeat signals obtained by a microwave reflectometer are not as clear as those observed in the ECG signals. It is therefore difficult to readily recover the HRV correctly and automatically from the microwave reflectometer signal. The purpose of this paper is to introduce different signal processing techniques to solve this problem.

Two novel elements are introduced in relation to the signal processing for the HRV reconfiguration in the microwave reflectometric measurement. In the first algorithm, the concept of interpreting the peak intervals in the cross-correlation

function between a measurement signal and a template signal is constructed by averaging periodic waveform in the measurement time. In the second one, the concept of calculating the time variation of the heartbeat frequency is estimated by the repetition of the maximum entropy method (MEM).

The contents of this paper are organized as follows. In Sec. II, the conventional method of the stress evaluation using an ECG is studied. The details of microwave reflectometry system, as applied to the measurement of human vital signals in noncontacting and noninvasive ways, are described in Sec. III. In Sec. IV, two different techniques for reconstruction of the HRV, by employing a cross-correlation method and MEM, are described and their validity is demonstrated in Sec. V. The numerical results are presented in Sec. VI and followed by conclusions.

## II. STRESS EVALUATION BASED ON ECG

In general, the evaluation of the stress is performed by analyzing the frequency spectrum of the HRV data. The HRV is inferred by interpreting the R-R intervals in an ECG data. A portion of the ECG data and the corresponding HRV for 180 s are shown in Figs. 1(a) and 1(b), respectively. The heartbeat interval is constantly fluctuating corresponding to autonomous nerve activity comprised of sympathetic and parasympathetic nerve activities. In the frequency spectrum of the HRV, the parasympathetic nerve activity appears in the spectral region of 0.15–0.45 Hz [high-frequency (HF) region, and both sympathetic and parasympathetic nerve activities appear in the region of 0.03–0.15 Hz [low-frequency (LF) region].<sup>4-6</sup> The peak ratio or area ratio of the power spectrum in the LF component to the HF component (LF/HF) is used to evaluate the stress. The sympathetic nerve activity increases in a stressful state and, on the other hand,

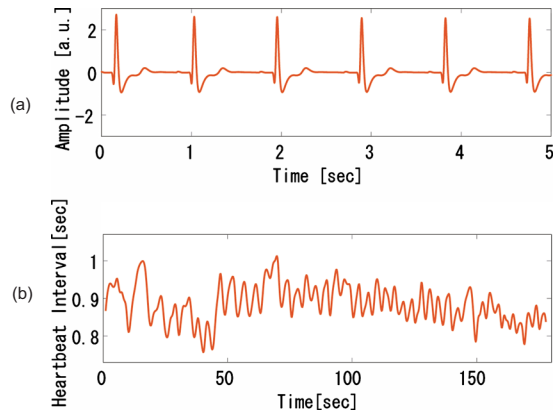


FIG. 1. (Color online) (a) ECG data. (b) HRV signal as a function of time.

the parasympathetic nerve activity increases in a relaxed state. The ratio (LF/HF) in a stressful state is larger than in a relaxed state.<sup>7–10</sup>

The fast Fourier transform (FFT), or the MEM, has been used in biomedical signal processing as a frequency analysis tool. The FFT is more often employed from the standpoint of the reproducibility of the power spectral density. When the FFT is employed, a HRV in excess of 100 s is required to ensure a frequency resolution in the LF and HF components of better than 0.01 Hz. In order to provide a reliable evaluation of the stress, the HRV for 180 s data interval is often employed. Additionally, the HRV must be interpolated at regular intervals in order to obtain the desired frequency spectrum. Differences in interpolation methods do not significantly influence the results, although various interpolation methods, such as the linear, the spline, etc. have been suggested. The most commonly employed interpolation interval is about 0.25 s.

The FFT frequency spectrum of the HRV for 180 s is shown in Fig. 2 where the HRV is interpolated at intervals of 0.25 s by the linear interpolation method. The characteristic peaks appear in the LF and the HF regions as shown in Fig. 2. Here it is noted that the evaluation of the stress by ECG has long been suggested as a reliable means to estimate mental stress.<sup>6,7</sup> However, as noted in the preceding, the stress evaluation method, using the ECG, seems to be unsuitable as a long-time monitoring the subject (the patient), as several electrodes are attached directly to the human body to acquire the ECG data. Specifically, there is some concern about the practical application of the ECG system to sick person and elderly person. Increased degree of inaccuracy in stress evaluation and sleep predictions are found in this method. Consequently, we propose using a noncontacting and noninvasive way to predict the evaluation of stress.

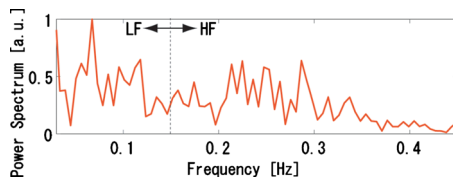


FIG. 2. (Color online) FFT spectrum of the HRV signal.

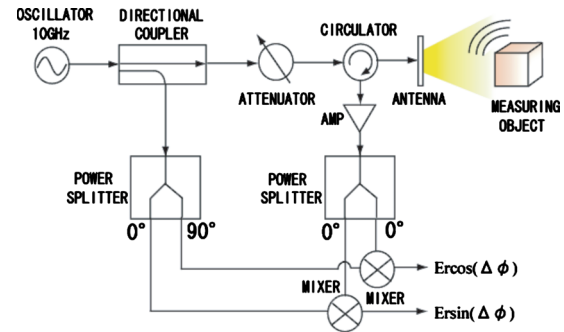


FIG. 3. (Color online) Schematic diagram of the microwave reflectometer.

### III. MICROWAVE REFLECTOMETER

There are many potential applications for a noninvasive technique to monitor heartbeat. Microwave radar reflectometry in the range of 2–10 GHz has been developed as a diagnostic tool to monitor heartbeat in Refs. 11–16. A block diagram of a phase sensitive microwave reflectometer is shown in Fig. 3. The output signal from the microwave oscillator (10 GHz, 100 mW) is fed into a directional coupler. The output is then attenuated by 20 dB and is irradiated onto the vicinity of human heart or the path of an artery in the thigh via a 16-element patch antenna array. The reflected wave from the human skin and/or from the surface of heart is picked up by the same antenna and then mixed with an unperturbed local oscillator wave in a quadrature phase detector. In the present system, the patch antenna used as transceiver is inserted into either the back rest of a seat for heartbeat signal monitoring or under the seat for detection from an artery in the thigh.

The quadrature phase detector provides two components in the mixer output,  $E_r \cos \Delta\phi$  and  $E_r \sin \Delta\phi$ , where  $E_r$  is the amplitude of the reflected wave and  $\Delta\phi$  is the phase difference between the reflected wave and the local oscillator wave. Thus,  $\Delta\phi$  and  $E_r$  are calculated numerically from Eqs. (1) and (2)

$$\Delta\phi = \tan^{-1} \left( \frac{E_r \sin \Delta\phi}{E_r \cos \Delta\phi} \right), \quad (1)$$

$$E_r = [(E_r \sin \Delta\phi)^2 + (E_r \cos \Delta\phi)^2]^{1/2}. \quad (2)$$

We can distinguish the amplitude and the phase difference of the reflectometer signals by detecting the above two components. The ac components of the phase difference include the periodic movement of the reflection layer due to the heart beat as well as random movement of the human body. The body movement, due to respiration, is only 1 cm or so at most; the motion due to heartbeat is typically only a fraction of a millimeter.<sup>17</sup> However, it is known that microwave reflectometers typically have a phase resolution of  $1/200$  fringe which corresponds to a spatial resolution of  $\lambda/400$ , where  $\lambda$  is the incident wavelength.<sup>16</sup> The wavelength corresponding to a carrier frequency of 10 GHz is 3.0 cm and, thus, the spatial resolution becomes  $75 \mu\text{m}$ . Therefore, the body movement due to the respiration and heartbeat can be detected easily.

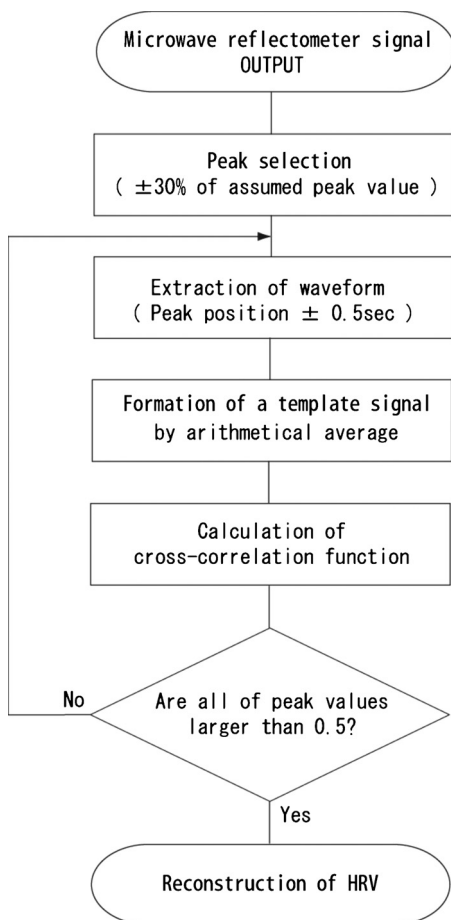


FIG. 4. Flowchart of the stress-evaluation algorithm.

To extract the heartbeat signal from the measurement signal, for example, the respiration signal is removed by a HPF with a cutoff frequency of 0.7 Hz. The spurious component of the reflected wave due to random movement of the human subject is difficult to be removed, though, since it has a wide frequency spectrum. Additionally, the heartbeat signal is very small and has low S/N ratio because the cardiac movement appears on the body surface through the bone and the connective tissue. Thus, the peak positions in the heartbeat signal obtained by a microwave reflectometer are not as clear as those observed in the ECG signals; this makes it difficult to infer the HRV correctly by interpreting the peak intervals of the microwave measurement signal without any data processing.

#### IV. SIGNAL PROCESSING FOR RECONSTRUCTION OF HRV

##### A. Cross-correlation technique

In this section, we propose a novel method to determine the heartbeat intervals clearly by applying a cross-correlation technique to the microwave reflectometer signals. An overview flowchart illustrating the proposed algorithm is shown in Fig. 4. The various steps/procedures are outlined as follows:

(i) The peak positions of the synchronized signals with the heartbeat are picked up and selected in the range

of  $\pm 30\%$  of an assumed peak value. It is noted that the body movement due to heartbeat is typically only a fraction of a millimeter, as stated above. Peak values of the phase difference signal corresponding to the heartbeat motion can therefore be estimated *a priori*. Peak values much larger than the estimated values are regarded as reflected waves caused by the random movement of the human body. On the other hand, peak values much smaller than the estimated value are caused by the small motion of other body tissues rather than the heart. Thus, the peak values corresponding to the heartbeat motion are selected from the microwave measurement signal. In this paper, we set up the estimated peak value  $\pm 30\%$  as the selection range according to our previous study.

(ii) The waveforms are picked out in the time length of the selected peak positions  $\pm 0.5$  s in series. The extraction time length is selected appropriately depending upon the measurement conditions. In the present system, the heart rate is assumed to be in the range of 30–120 beats per minute (bpm). It is desired that the template signal contains characteristics of one heartbeat waveform. If the template signal does not contain characteristics of one heartbeat waveform, the peak intervals of the cross-correlation function waveform become unclear. In the microwave measurement signal, one heartbeat waveform is characterized as a bell-shaped waveform, with more details presented in Sec. V. In order to capture the characteristics of one heartbeat waveform, it is necessary that the length of the template signal is selected in the range of  $1/2$ – $2$  periods around a central peak. For example, if the length of the template signal is selected at 0.5 s before and after the central peak, the characteristics of one beat waveform of heartbeat signals at 30–120 bpm are captured. A heart rate span of 30–120 bpm sufficiently covers the heart rate for a seated human subject, since it is typically in the range of 45–90 bpm, i.e., 0.75–1.5 Hz.<sup>17</sup>

Additionally, it is noted that an appropriate number of extracted signals is necessary for correct construction of the template signal. If the number is too small, the quality of the template signal becomes low as it is difficult to remove the influence of various noise (spurious) components in the measurement signal by averaging procedures. However, if the number is too large, the quality can also be degraded since the heart rate of the human subject changes a lot when his mental status is unstable. In the present experiment, the number 30 is selected based on empirical experience. The template signal is inferred by the first 30 of extracted signals.

(iii) A template signal is formed by the arithmetic average of the extracted waveforms.

(iv) The cross-correlation function between the template and the measurement signal is calculated. The cross-correlation function that represents the reliability of the heartbeat interval can be written as



$$R(m) = \frac{(K(k_{M1}, k_{M2}, \dots, k_{MN}), L(l_1, l_2, \dots, l_N))}{\|K(k_{M1}, k_{M2}, \dots, k_{MN})\| \cdot \|L(l_1, l_2, \dots, l_N)\|}, \quad (3)$$

where  $K(k_{M1}, k_{M2}, \dots, k_{MN})$  is the microwave measurement signal,  $L(l_1, l_2, \dots, l_N)$  is the template signal,  $m\Delta T$  is the heartbeat interval,  $\Delta T$  is the sampling period,  $M$  is the arbitrary data point of the microwave measurement signal, and  $N$  is the data length of the template signal. The signs of  $(\cdot)$  and  $\|\cdot\|$  indicate the symbols of inner product and norm, respectively.

- (v) If any of the peak values in the cross-correlation function fall below 0.5, the cross-correlation functions are calculated repeatedly as the second or the third cross-correlation functions. This method works well for the case when large noise components are mixed with the reflectometer signals which make it difficult to identify the peak intervals in the first cross-correlation function.
- (vi) The HRV is obtained by interpreting the peak intervals in the cross-correlation function.

## B. MEM technique

The time variation of the heartbeat intervals can be regarded as the short-term time variation of the heartbeat frequency. In this section, the time variation of the heartbeat frequency is evaluated by applying the MEM repeatedly over the short term. The time window is shifted step by step along the temporal axis. The HRV can then be reconstructed once the value of the heartbeat interval is calculated by the inverse of the heartbeat frequency. The MEM is an effective tool for estimating the frequency spectrum at a small data window and has a much higher frequency resolution than the FFT.<sup>18,19</sup> In the case of the FFT, the spectrum estimation at a small data window has limitations because the frequency resolution is the inverse of the time window for the analysis.

In the MEM analysis, the autoregressive model of the observational data is estimated first and then the spectrum estimation is performed on the basis of it. The autoregressive model is given by

$$x_k = - \sum_{i=1}^m a_{mi} x_{k-i} + n_k, \quad (4)$$

where  $x_k$  is the observed time-series of data interval,  $n_k$  is the stationary white noise which is independent from  $x_l (l < k)$ ,  $m$  is the order of the autoregressive model, and  $a_{mi}$  is the autoregressive coefficient at the model order  $m$ . We now define the autocorrelation function of the time-series data  $x_k$  as

$$R_i = R(i\Delta t) \equiv E\{x_k x_{k-i}\}, \quad (5)$$

where  $E\{\cdot\}$  is the expectation value. The autocorrelation function at lag 0 is shown as

$$R_0 = E\{x_k^2\} = - \sum_{i=1}^m a_{mi} R_i + E\{n_k^2\}. \quad (6)$$

Since  $n_k$  and  $x_l (l < k)$  are independent to each other, the autocorrelation function at each lag is organized by

$$\begin{bmatrix} R_0 & R_1 & \cdots & R_m \\ R_1 & R_0 & \cdots & R_{m-1} \\ \vdots & \vdots & \ddots & \vdots \\ R_m & R_{m-1} & \cdots & R_0 \end{bmatrix} \begin{bmatrix} 1 \\ a_{m1} \\ \vdots \\ a_{mm} \end{bmatrix} = \begin{bmatrix} P_m \\ 0 \\ \vdots \\ 0 \end{bmatrix}, \quad (7)$$

where  $P_m$  is the variance of the stationary white noise. By applying the Wiener–Khinchine formula<sup>20</sup> to Eq. (4), the relationship between the autoregressive model  $\{a_{kj}\}$  and the power spectrum  $S(\omega)$  is shown as

$$S(\omega) = \frac{P_m \Delta t}{|1 + \sum_{i=1}^m a_{mi} e^{-j\omega i \Delta t}|^2}. \quad (8)$$

In the MEM, the model order is generally unknown. If the model order is too low, the estimated spectrum is smoothed and the spectrum peak, which should be observed, may not appear. On the other hand, if the model order is too high, many spurious peaks often appear in the estimated spectrum. Thus, the optimum value of the model order is very important in the MEM analysis.

The final prediction error and Akaike's information criteria have been suggested for the estimation of the optimum model order.<sup>21,22</sup> Since the model order selected by these techniques is typically very small, however, the estimated spectrum is smoothed significantly. The spectrum peaks are therefore not found in the desired frequency range. These techniques in fact are not adequate for resolution of the multiple-period structure. If the observed data have the multiple-period structure and only a part of frequency domain is focused on, for example, the estimation of the heartbeat frequency, these techniques may not work properly. In this case, we estimated the optimum model order from the simulation model of the heartbeat signal; the details are presented in Appendix A. Accordingly, we selected the optimum model order as 870.

The heartbeat frequency is estimated by finding the largest peak value over the frequency span of 0.7–1.55 Hz (42–98 bmp) after calculating the power spectrum of some data windows by MEM. Here, the frequency span of 0.7–1.55 Hz sufficiently covers the range of heartbeat frequency range of 0.7–1.5 Hz for a human subject at sitting rest.

If the analyzing data window is selected to be excessively long, the time response of the heartbeat intervals becomes sluggish in the HRV while the reliability of the estimation increases. This could exert a negative influence upon the estimation of the ratio LF/HF. Consequently, we investigated the relation between the length of the data window, the accuracy of the ratio (LF/HF) and the details are presented in Appendix B. Accordingly, 2.5 s is selected as the optimum length of the data window for the MEM analysis.

In addition, 0.25 s is selected as the shift quantity of the data window. It is equal to the interpolated value of the HRV reconstructed by the ECG. Unlike the nonstationary spectrum analysis techniques, the MEM is highly regarded as a reliable stationary spectrum analysis technique where the consistency of the signal in the data window is achieved. As the correspondence relationship between the data windows is ignored, some spectrum estimation errors due to the selected data window appear as the fluctuation with a period of 0.25 s which is equivalent to 4 Hz in frequency in the HRV signal.

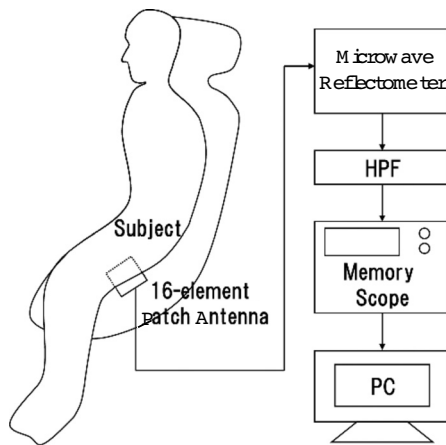


FIG. 5. Experimental setup.

This is not a problem, however, for the evaluation of the stress because the spectrum estimation error between data windows is very small and its fluctuation does not extend over the frequency region of the LF and the HF.

For these reasons, the time variation of the heartbeat frequency is estimated by repeatedly applying the MEM at the 2.5 s data window which is then shifted by 0.25 s along the temporal axis.

## V. EXPERIMENTAL RESULTS AND DISCUSSION

### A. Equipment setup

Figure 5 shows a schematic diagram of the measurement arrangement in which the subject is sitting on a chair. We selected the thigh arbitrarily, as an irradiation point of microwave, since its skin movement is largely due to the existence of thick artery, while it should be small during respiration. We installed the 16-element patch antenna array into the seat of a chair under the left thigh of the human subject. The back of the chair can also be selected as the antenna position since it is close to the heart.

The analog output from the microwave reflectometer is fed to a HPF in order to remove the respiratory components. The output signal is then converted into a digital signal by a high-resolution (16 bits) memory scope. The sampling frequency of 30–300 Hz is needed to capture the characteristics of the heartbeat period.<sup>15,23</sup> In the present experiment, a sampling frequency of 1000 Hz is chosen; this is much larger than 30–300 Hz. The digitized signals are fed into a computer. Since the quadrature phase detector provides  $\sin \Delta\phi$  and  $\cos \Delta\phi$  (I/Q) components, the phase difference  $\Delta\phi$  between the reflected wave and the local oscillator wave is calculated from Eq. (1). Afterward, the evaluation of stress is performed by applying the proposed algorithms to the phase difference signals. The measurement for the ECG is performed simultaneously in each experiment.

### B. Stress evaluation 1: Static environment

In the first experiment, the stress evaluation methods are applied to a person in both relaxed state and stressful states. The flash mental calculation is used to put stress on a person where the figures are displayed continuously on a monitor

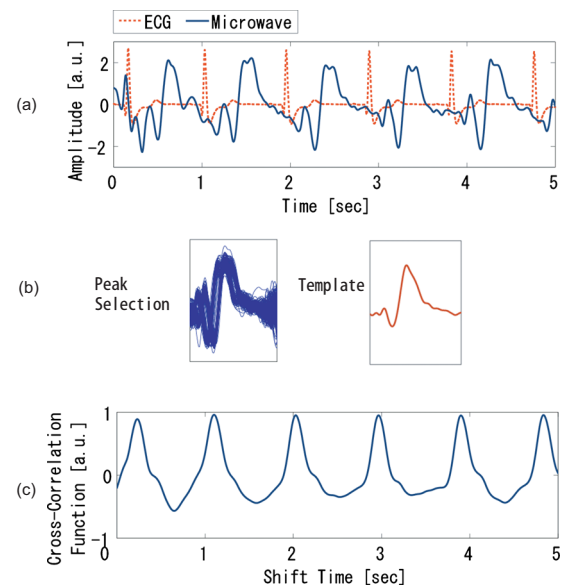


FIG. 6. (Color online) (a) Comparison between the microwave reflectometer signal and the ECG, (b) selected peak waveforms and a template, and (c) calculated cross-correlation function.

before the subject's head.<sup>24,25</sup> The heartbeat measurement by a microwave reflectometer is applied to the person who is in a relaxed or the stressful state for 180 s. The above two proposed methods are applied to reconstruct the HRV signals. The ratio (LF/HF) is then calculated by applying a FFT to the HRV signals in the time interval of 180 s. For comparison, the ECG data are measured at the same time in each state. The corresponding ratio (LF/HF) is calculated by the conventional stress evaluation method.

Figure 6(a) shows the time evolutions of the microwave reflectometer signal and the ECG signal of the person in the relaxed state. Note that the time interval of the periodic signal is in good agreement between the two signals. This implies that the heart beat can be obtained correctly from the microwave reflectometry measurements. The cross-correlation function, calculated by using the first technique, is shown in Fig. 6(b). It is shown that the determination of the peak intervals becomes much easier compared to the original signal as shown in Fig. 6(a).

Figure 7 shows the subsets of the HRVs reconstructed by interpreting the peak intervals in the ECG data, the original microwave reflectometer signal and the cross-correlation

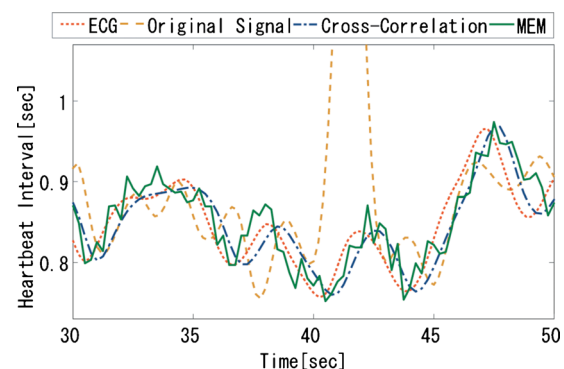


FIG. 7. (Color online) HRV reconstructed from each signal.

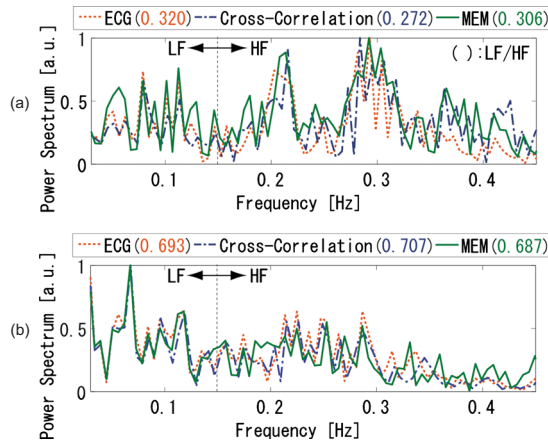


FIG. 8. (Color online) (a) FFT spectrum of the HRV in relaxed state and (b) FFT spectrum of the HRV in the stressful state.

function, together with the one reconstructed by applying the MEM technique to the original signal. Note that large discrepancy of the HRV data often occurs between the original microwave reflectometer signal and the ECG signal as shown in Fig. 7, since large peaks due to the body motion will be picked up rather than the peaks due to the heart beat without any processing. The HRVs calculated by the two proposed methods agree well with the data measured by the ECG method, comparing only the unprocessed reflectometer signal. Additionally, the HRV calculated by the MEM contains a periodic noise component compared to that calculated by the cross-correlation technique. This might be caused by some spectrum estimation errors between data windows which appear as the fluctuation by 0.25 s (4 Hz in frequency) in the HRV. The estimated error of the HRV due to the spectrum estimation error, however, is very small, i.e., about several percent of the HRV values. Thus, the fluctuation of estimation errors is not a problem for the evaluation of the stress as described in Sec. IV. Therefore, it is understood that the HRV is reconfigured correctly by using two proposed methods.

The frequencies of the HRVs calculated by two proposed methods, and the ECG in the relaxed state, are analyzed, respectively. Generally, it is known that the individual variability of the ratio of LF/HF is about  $\pm 30\%$ .<sup>7,8</sup> If the spectral shapes of the HRVs are similar, and the ratio LF/HFs can be estimated by the two proposed methods in the range of  $\pm 30\%$  as compared to the ECG, it could be argued that the estimation of stress is successful.

The comparative results are presented in Fig. 8(a) for a relaxed state. The corresponding results for a stressful state are shown in Fig. 8(b). In both figures, normalized data are presented. The frequency spectra of the HRVs calculated by applying two proposed methods to the microwave measurement are nearly correspondence to the data calculated by the ECG. The ratios of LF/HF obtained by the two proposed methods are consistent in the range of  $\pm 30\%$  compared to that obtained by the ECG in each state. Here, the ratio (LF/HF) is obtained from the area values of the spectrum. Additionally, it is understood that the flash mental calculation puts stress on the person since the LF/HF value in the stressful state is about twice that in the relaxed state. These results

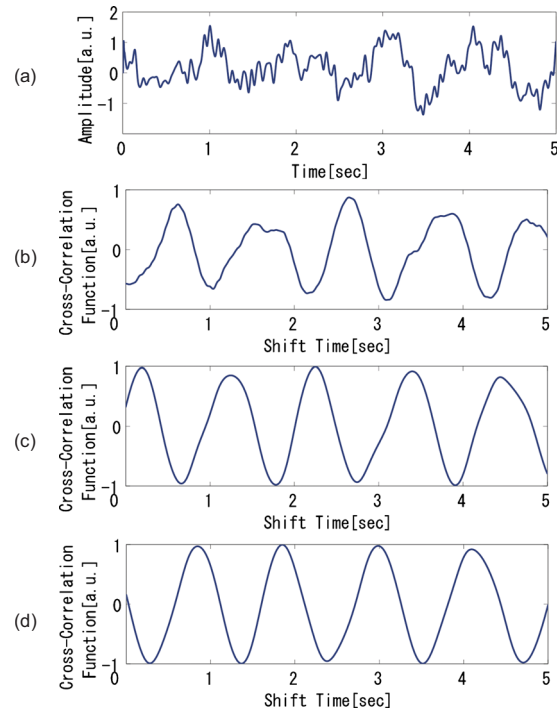


FIG. 9. (Color online) (a) Time evolution of the microwave reflectometer signal, (b) the first cross-correlation function, (c) the second cross-correlation function, and (d) the third cross-correlation function.

show that the evaluation of stress can be performed by applying the proposed methods to the microwave reflectometer signal similar to the ECG.

### C. Stress evaluation 2: Nonstatic environment

In the second experiment, the above evaluation methods of stress are applied to a person in a nonstatic environment. It is not always true that the stress evaluation is applied to a static environment at all times. In order to test this, the measurements were carried out in a car. The stress evaluation procedures were carried out when the engine vibration is on. The heartbeat is measured by using a microwave reflectometer that is applied to the person who is sitting in the driver's seat.

The two proposed methods are applied to the reconstruction of the HRV. The LF/HF value is then calculated by applying the FFT to the HRV for 180 s. For comparison, the ECG data are measured at the same time in each state and the LF/HF value is calculated.

In the nonstatic environment, the microwave reflectometer signal includes various noise (spurious) components due to random movements of the body surface, thus making it harder to detect the heartbeat interval. Figure 9(a) shows an example of a measurement with such noise components. In the following section, we will investigate whether the evaluation of stress is possible in the nonstatic environment by the two proposed methods.

First, the cross-correlation technique is applied to the microwave reflectometer signal and is shown in Fig. 9(b). Here, the higher-order cross-correlation functions are calculated repeatedly, as shown in flow chart in Fig. 4, and when the peak values drop below 0.5 in the first cross-correlation



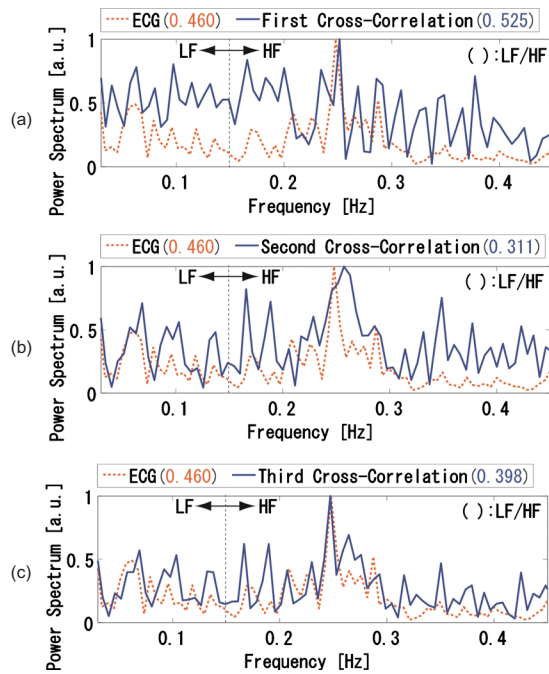


FIG. 10. (Color online) FFT spectra of the HRV obtained by the cross-correlation technique and the ECG signal: (a) first, (b) second, and (c) third cross-correlation.

function. The results of the second and the third order cross-correlation functions are shown in Figs. 9(c) and 9(d). As shown, the peak intervals of the waveform become clear by the repeated calculation of the cross-correlation functions. Figure 10 shows the frequency spectra of the HRV reconstructed by the each-order of cross-correlation function, together with those obtained from the ECG signals. In Fig. 10(a), though the ratio LF/HF consists in the range of  $\pm 30\%$  compared to that obtained by the ECG, the spectral shapes of the HRVs are not similar at all. This inconsistency in comparison data (after first correlation function) reflects the inaccuracy in the estimation of stress. The repeated calculations of the cross-correlation make the frequency spectrum of the HRV more consistent with that obtained by the ECG. The spectral shapes of the HRV using the third cross-correlation function is now nearly equal to that by the ECG and the ratio LF/HF consists in the range of  $\pm 30\%$  compared to that obtained by the ECG.

Second, the MEM technique is applied to the microwave reflectometer signal for the reconstruction of the HRV. Figure 11 shows the frequency spectra of the HRV calculated by the MEM technique, together with those obtained from the ECG signals. In Fig. 11, the spectrum forms of both sides have a well similarity. Additionally, the evaluation of the ratio

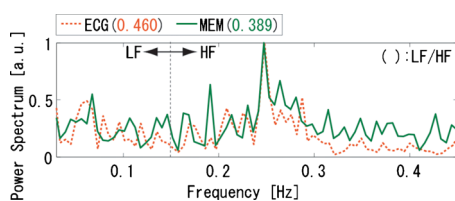


FIG. 11. (Color online) FFT spectra of the HRV obtained by the MEM technique and the ECG signal.

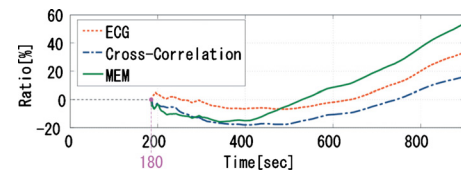


FIG. 12. (Color online) Time change rates of the LF/HF.

LF/HF using the MEM technique consists in the range of  $\pm 30\%$  compared to that by the ECG.

These results show that the evaluation of stress can be performed by applying the proposed methods (two different approaches) to microwave reflectometer signals similar to ECGs even in the case of a nonstatic environment. In this regard, the repetitive operations of the cross-correlation function add a considerable amount of calculation and complexity in the signal processing. It is possible to plot the data of the HRV every 2 s in the MEM technique. Therefore, when a short-time or real-time stress evaluation is necessary in a nonstatic environment, the MEM technique will be indispensable.

### D. Stress evaluation 3: Long-time monitoring

In this section, the time fluctuation of stress is monitored over a longer duration. In the long term stress monitoring, the stress situation is evaluated by the time change rate of the ratio LF/HF value. This ratio LF/HF is not a constant and varies between individuals.<sup>9</sup> The heartbeat measurement by the microwave reflectometer is applied to the person who is in a relaxed state for 900 s. The two methods are applied for the calculation of the HRV. The LF/HF value is calculated by applying FFT to the HRV for 180 s. The time change of the LF/HF for 180–900 s is calculated by shifting the data window by 1 s along the temporal axis. The time change rate for the LF/HF value for 180–900 s is then calculated on the basis of the LF/HF for the first 180 s. For comparison, the ECG data are measured at the same time and the time change rate of the LF/HF for 180–900 s is calculated in a similar way.

Figure 12 shows the time change rates of the LF/HF calculated by the two proposed methods for the microwave measurement, together with that obtained from the ECG. The time change rates of the LF/HF, calculated by the two proposed methods, are qualitatively in agreement with that obtained from the ECG. This result shows that long-term stress monitoring can be performed by applying two proposed methods to microwave reflectometer signal as well as to ECG signal.

### E. Comparative discussion

It is demonstrated that the two proposed methods work very well in different situations, such as static and nonstatic environments. However, they differ greatly in computational time and the complexity of signal processing. The different criteria for selecting the individual method are discussed below.

If the stress evaluation is in a nonstatic environment, the MEM technique works better than its counterpart. The repetitive operations of the cross-correlation function will re-



sult in a large amount of calculations and complexity to the evaluation process. The MEM technique enables the evaluation in only one calculation in any given environment.

On the other hand, we have to choose the cross-correlation technique if further evaluation of the stress is required or not, such as the coefficient of variation of R-R intervals (CVRR) in addition to the LF/HF value. The CVRR is a ratio of the standard deviation of heartbeat intervals. The values and the heartbeat intervals are obtained only by interpreting the peak intervals in the waveform.

## VI. CONCLUSION

In this work, we proposed two new signal processing techniques for microwave reflectometer sensing applications that enable estimation of mental stress from a measurement of body dynamic motion. Two algorithms, based on cross-correlation techniques and the MEM, are studied to reconstruct the HRV correctly and automatically from low-S/N microwave reflectometer signals. These techniques greatly improve the accuracy of the HRV reconstruction and enable the stress evaluation by microwave reflectometers.

Two signal processing techniques were proposed and applied to a microwave reflectometric measurement using live subjects. These procedures can be used as follows: to detect the existence or nonexistence of the stress; to detect, stress evaluation in nonstatic environment; for long-term stress monitoring.

The two techniques are applicable to any case, if the computation time and the complexity of the processing are not constraints. The selection of the processing techniques will depend on the types of measurement and environments. The results are presented for the two different algorithms and found to be consistent with ECG data. In this work, we primarily intended to introduce new concepts in signal processing techniques to evaluate stress in both static and nonstatic environments. However, practical issues, such as personal dependence related to age and different health conditions, were not considered. We would like to explore these additional issues in subsequent work.

## ACKNOWLEDGMENTS

This work is partly supported by the Grant-in-Aid for Scientific Research, the Ministry of Education, Science, Sports and Culture (Grant No. 20360186), and by the Grant for Practical Application of University R&D Results under the Matching Fund Method, NEDO.

## APPENDIX A: SELECTION OF OPTIMUM MODEL ORDER

In the MEM, the estimation of the optimum model order is necessary to correctly detect heartbeat frequencies. In the following section, the optimum model order is estimated by a simulation using a heartbeat signal model suggested by Morgan and Zierdt.<sup>26</sup>

For a heartbeat signal component, a characteristic analog pulse shape  $p_H(t)$  that is generated at discrete times  $t$  is assumed by

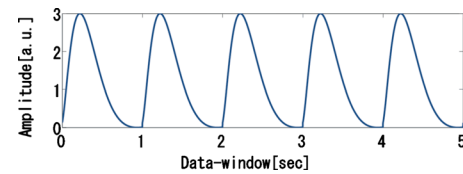


FIG. 13. (Color online) Heartbeat signal model.

$$p_H(t) = e^{-t/\tau} + \left[ \left( \frac{\sqrt{2}}{\omega_0\tau} - 1 \right) \sin \frac{\omega_0 t}{\sqrt{2}} - \cos \frac{\omega_0 t}{\sqrt{2}} \right] e^{-\omega_0 t / \sqrt{2}}. \quad (\text{A1})$$

The analog pulse shape introduced here has an exponential function  $e^{-t/\tau}$ , with time constant  $\tau$ , filtered by a second-order Butterworth (critically damped) filter with cutoff frequency  $f_0$ . The simplistic motivation for this model is that when the heart or artery is pumped, it is likely to impart a short impulsive motion that is subsequently filtered by the bone and tissue and then sensed by the body surface.  $p_H$  is then periodically repeated at the intervals of  $1/f_H$  and sampled at  $f_s$  to obtain the discrete heartbeat signal

$$x_H(n) = p_H \left( \frac{n}{f_s} - \left[ \frac{n}{f_s} \right] \frac{1}{f_H} \right), \quad (\text{A2})$$

where,  $f_H$  is the heartbeat frequency in hertz (heart rate of  $f_H$  in bmp) and  $[x]$  is defined as the greatest integer less than or equal to  $x$ . In addition,  $f_s$  is the sampling frequency and  $t$  can be rewritten as  $t = n/f_s$ ,  $n = 1, 2, \dots, N$ . Thus, the samples  $p_H(n/f_s)$  are taken sequentially until  $n/f_s$  reaches the heart-rate period  $1/f_H$ ; at that point the next pulse is started and so on. This result provides the heartbeat signal model. In this paper, we select  $\tau = 0.05$  s and  $f_0 = 1$  Hz for pulse parameters and made the heartbeat signal model with  $N = 5000$  samples (5 s) at a sampling rate of  $f_s = 1000$  Hz, where 1000 Hz is equal to the sampling frequency in the real measurement. Figure 13 shows the heartbeat signal model at the heartbeat frequency  $f_H = 1$  Hz, as an example, where one can clearly see the repeated Butterworth-like pulse shapes.

The estimation of the optimum model order is performed by the following procedures.

- (1) The 48 sets of heartbeat signal models with data window of 5 s are made by changing the heartbeat frequency  $f_H$  by 0.167 Hz from 0.7 Hz to about 1.5 Hz in Eq. (4). The frequency range of 0.7–1.5 Hz corresponds to the range of heartbeat frequency for a seated human subject, where the frequency step 0.0167 Hz is equivalent to the 1 bmp of the heartbeat.
- (2) The 49 sets of data windows are extracted repeatedly by increasing the length of extraction by 0.1 s from 0.1 to 5.0 s in each heartbeat signal models.
- (3) By increasing the model order by 10 from 1 to the maximum, the estimation of heartbeat frequency by the MEM is applied to the  $48 \times 49$  data at each heartbeat signal models and each length of data window. At each data point, the maximum model order is equivalent to the length of data window. Here, the heartbeat frequency is estimated by finding the largest peak in the frequency

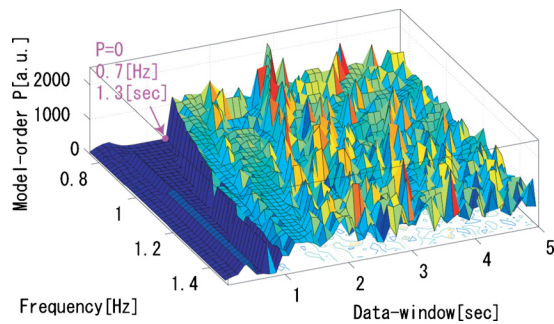


FIG. 14. (Color online) Relationship among the heartbeat frequency, the length of data window, and the estimated model order.

range of 0.7–1.5 Hz. If every peak cannot be found in every model order, the estimated model order is shown as 0.

- (4) The model order is selected as “the estimated model order,” at which the estimated error of the heartbeat frequency is minimum.

Figure 14 shows the relationship among the heartbeat frequency, the length of data window, and the estimated model order. The length of data window over 1.4 s is required to estimate every heartbeat frequency for 0.7–1.5 Hz. The estimated model orders are then averaged every length of data window; the result is shown in Fig. 15. It is noted that about 870 model order is optimum in case of selecting each length of data window.

## APPENDIX B: SELECTION OF DATA WINDOW

We investigated the relationship between the length of data window and the accuracy of the LF/HF using several sets of real data in the following section. We used five sets of measurement signals obtained by a microwave reflectometer applied to a person in a relaxed state for 180 s simultaneously measured by an ECG.

If the data window is selected to be too long, the time response of the heartbeat intervals becomes sluggish in the HRV, while the reliability of the estimation increases. This could exert a negative influence upon the estimation of the LF/HF. The optimum length of the data window is investigated by the following procedures.

- (1) The 36 sets of the HRVs are reconstructed by increasing the length of the data window by 0.1 s from 1.4 to 5.0 s at each measurement signals. It has been simulated that the length of the data window over 1.4 s is required to estimate the heart rate of the seated person in Appendix A.

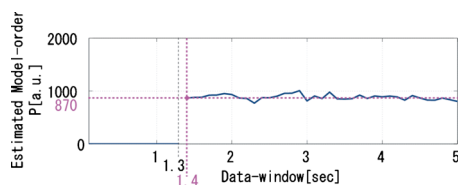


FIG. 15. (Color online) Relationship between the length of data window and the average of the estimated model order.

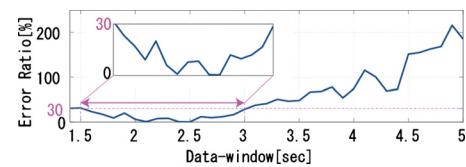


FIG. 16. (Color online) Relationship between the length of data window and the average of standardized error rates of LF/HF values.

- (2) The error rates of the LF/HF are estimated from each HRV at each measurement signal. Here, the error rate is calculated by comparing with the LF/HF from the ECG.
- (3) The minimum estimate error rate at each measurement signals is standardized as 0. This is caused by removing the estimate error, due to the measurement quality at each measurement signal, not due to the length of the data window. At each datum, the maximum model order is equivalent to the length of the data window.
- (4) The standardized error rates of the LF/HF at each length of the data window are averaged using five sets of microwave measurement signals.

Figure 16 shows the relationship between the length of the data window and the average of the standardized error rates of LF/HF. In Fig. B1, the LF/HF can be estimated with higher accuracy (less than 30%) if the data window is selected for 1.5–3.0 s. In this paper, we selected 2.5 s as the length of the data window. This length has the smallest error ratio as shown in Fig. 16.

- <sup>1</sup>E. Landenberger-Leo, *Med. Pr* **37**, 347 (1986).
- <sup>2</sup>M. F. Hilton, R. A. Bates, K. R. Godfrey, M. J. Chappell, and R. M. Cayton, *Med. Biol. Eng. Comput.* **37**, 760 (1999).
- <sup>3</sup>K. C. Bilchick, B. Fetics, R. Djoukeng, S. G. Fisher, R. D. Fletcher, S. N. Singh, E. Nevo, and R. D. Berger, *Am. J. Cardiol.* **90**, 24 (2002).
- <sup>4</sup>M. Malik, *Circulation* **93**, 1043 (1996).
- <sup>5</sup>L. Duvnjak, S. Vuckovic, N. Car, and Z. Metelko, *J. Diabetes Complications* **15**, 314 (2001).
- <sup>6</sup>U. Wiklund, M. Akay, and U. Niklasson, *IEEE Eng. Med. Biol. Mag.* **16**, 113 (1997).
- <sup>7</sup>M. Takada, H. Takada, and A. Katayama, *Health Eval. Promo.* **32**, 504 (2005).
- <sup>8</sup>M. Takada, T. Ebara, and Y. Sakaki, *HEP* **35**, 373 (2008).
- <sup>9</sup>Y. Yoshida, K. Yokoyama, and N. Ishii, *IEEJ Trans. EIS.* **126**, 1441 (2006).
- <sup>10</sup>R. Tsuda, *Bulletin of School of Information Science* (Kyushu Tokai University, Kumamoto, 2003), Vol. 13, pp. 3–29.
- <sup>11</sup>J. C. Lin, *Proc. IEEE* **63**, 1530 (1975).
- <sup>12</sup>P. C. Pedersen, C. C. Johnson, C. H. Durney, and D. G. Bragg, *IEEE Trans. Biomed. Eng.* **BME-23**, 410 (1976).
- <sup>13</sup>D. W. Griffin, *Microwave J.* **21**, 69 (1978).
- <sup>14</sup>J. C. Lin, J. Kiernicki, M. Kiernicki, and P. B. Wollschlaeger, *IEEE Trans. Microwave Theory Tech.* **27**, 618 (1979).
- <sup>15</sup>K.-M. Chen, D. Misra, H. Wang, H.-R. Chuang, and E. Postow, *IEEE Trans. Biomed. Eng.* **BME-33**, 697 (1986).
- <sup>16</sup>N. Tateishi, A. Mase, L. Bruskin, Y. Kogi, N. Ito, T. Shirakata, and S. Yoshida, Proceedings of the 2007 Asia Pacific Microwave Conference, Bangkok, 2007, pp. 2151–2153.
- <sup>17</sup>A. D. Droitcour, Ph.D. thesis, Stanford University, 2006.
- <sup>18</sup>J. P. Burg, Proceedings of the 37th Annual International Meeting, Society of Exploration Geophysics, Oklahoma, October 1967.
- <sup>19</sup>See <http://cmm.cit.nih.gov/maxent/letsgo.html> for the MEM of data analysis.

- <sup>20</sup>J. S. Bendat and A. G. Piersol, *Random Data: Analysis and Measurement Procedures* (Wiley-Interscience, New York, 1971).
- <sup>21</sup>H. Akaike, *Ann. Inst. Stat. Math.* **21**, 243 (1969).
- <sup>22</sup>H. Akaike, *Ann. Inst. Stat. Math.* **21**, 407 (1969).
- <sup>23</sup>B. Lohman, O. Boric-Lubecke, V. M. Lubecke, P. W. Ong, and M. M. Sondhi, Proceedings of the 23rd Annual International Conference of the IEEE Engineering in Medicine and Biology Society, Istanbul, 2001, pp. 3359–3362.
- <sup>24</sup>P. Burbaud, P. Degreze, P. Lafon, J. M. Franconi, B. Bouligand, B. Bioulac, J. M. Caille, and M. Allard, *J. Neurophysiol.* **74**, 2194 (1995).
- <sup>25</sup>H. Mizuhara, L-Q. Wang, K. Kobayashi, and Y. Yamaguchi, *NeuroReport* **15**, 1233 (2004).
- <sup>26</sup>D. R. Morgan and M. G. Zierdt, *Signal Process.* **89**, 45 (2009).